Published OnlineFirst August 19, 2016; DOI: 10.1158/0008-5472.CAN-16-0179

Tumor and Stem Cell Biology

Cancer Research

Impaired Planar Germ Cell Division in the Testis, Caused by Dissociation of RHAMM from the Spindle, Results in Hypofertility and Seminoma

Huaibiao Li[1], Lucien Frappart[1,2], Jürgen Moll[3], Anne Winkler[1], Torsten Kroll[1], Jana Hamann[1], Iris Kufferath[4], Marco Groth[1], Stefan Taudien[1], Moritz Schütte[5], Marie-Laure Yaspo[6], Heike Heuer[1], Bodo M.H. Lange[5,6], Matthias Platzer[1], Kurt Zatloukal[4], Peter Herrlich[1,3], and Aspasia Ploubidou[1]

Abstract

Hypofertility is a risk factor for the development of testicular germ cell tumors (TGCT), but the initiating event linking these pathologies is unknown. We hypothesized that excessive planar division of undifferentiated germ cells promotes their self-renewal and TGCT development. However, our results obtained from mouse models and seminoma patients demonstrated the opposite. Defective planar divisions of undifferentiated germ cells caused their premature exit from the seminiferous tubule niche, resulting in germ cell depletion, hypofertility, intratubular germ cell neoplasias, and seminoma development. Oriented divisions of germ cells, which determine their fate, were regulated by spindle-associated RHAMM—a function we found to be abolished in 96% of human seminomas. Mechanistically, RHAMM expression is regulated by the testis-specific polyadenylation protein CFIm25, which is downregulated in the human seminomas. These results suggested that spindle misorientation is oncogenic, not by promoting selfrenewing germ cell divisions within the niche, but by prematurely displacing proliferating cells from their normal epithelial milieu. Furthermore, they suggested RHAMM loss-of-function and spindle misorientation as an initiating event underlying both hypofertility and TGCT initiation. These findings identify spindle-associated RHAMM as an intrinsic regulator of male germ cell fate and as a gatekeeper preventing initiation of TGCTs. *Cancer Res; 76(21); 6382–95. ©2016 AACR.*

Introduction

Testicular germ cell tumors (TGCT) are cancers with metastatic potential and of rising incidence (1). Hypo/infertility is one of the main risk factors for adult TGCT development and can precede tumorigenesis by several years (2, 3). Despite extensive research, the etiology of TGCT is not well understood. Loss of heterozygosity, allelic imbalance, and genome-wide association studies (GWAS) have identified several loci and genes conferring TGCT susceptibility; however, most of them are not functionally characterized (4–7). On the basis of these and other data, models of TGCT development have been proposed (8) but the initiating event behind these cancers remains unknown.

The understanding of cancer-initiating events is linked to the identification of cells of origin, a very challenging task in solid tumors. TGCT offer a significant advantage in such investigations, because their cells of origin are known to be the germline stem cells—gonocytes or spermatogonia (8). Seminomas are the most common type of pure TGCT, developing from the precursor lesion intratubular germ cell neoplasia (IGCN; ref. 8).

In contrast to other tissues, where daughter cells enter differentiation early, progenitor cells of the testis proliferate extensively. This highly proliferating nature of spermatogonia implies that the driving event for somatic tumors, that is, uncontrolled proliferation, might not apply to TGCTs, as TGCTs occur at low frequency in relation to the overall rate of proliferation in the testis (9). Rather, inhibition of spermatogonial differentiation is thought to induce seminoma development, a notion supported by a mouse model that exhibits increased self-renewal of spermatogonia because of an overexpression of GDNF (10). Nonetheless, the mechanisms and molecules regulating the balance between germ cell (GC) renewal and differentiation in testis remain to be unraveled (11).

Self-renewal and differentiation of stem cells is maintained by symmetric and asymmetric divisions, which are dictated by spindle orientation (12). Defective spindle orientation has been associated with oncogenesis in several systems, but definitive

[1]Leibniz Institute on Aging - Fritz Lipmann Institute, Jena, Germany. [2]INSERM, Oncogenèse et Progression Tumorale, Université Claude Bernard Lyon I, Lyon, France. [3]Forschungszentrum Karlsruhe, Institut für Toxicologie und Genetik, Karlsruhe, Germany. [4]Christian Doppler Laboratory for Biospecimen Research and Biobanking Technologies, Institute of Pathology, Medical University of Graz, Graz, Austria. [5]Alacris Theranostics GmbH, Berlin, Germany. [6]Max-Planck Institute for Molecular Genetics, Berlin, Germany.

Note: Supplementary data for this article are available at Cancer Research Online (http://cancerres.aacrjournals.org/).

L. Frappart, J. Moll, and A. Winkler contributed equally to this article.

Current address for J. Moll: Boehringer-Ingelheim RCV & Co KG, Vienna, Austria; current address for A. Winkler, Department of Neuropathology, Georg-August-University Göttingen, Göttingen, Germany; and current address for H. Heuer, Leibniz Research Institute for Environmental Medicine, Düsseldorf, Germany.

Corresponding Author: Aspasia Ploubidou, Leibniz Institute on Aging - Fritz Lipmann Institute, Beutenbergstrasse 11, Jena D-07745, Germany. Phone: 49-3641-656468; Fax: 49-3641-656335; E-mail: aspasia.ploubidou@leibniz-fli.de

doi: 10.1158/0008-5472.CAN-16-0179

Published OnlineFirst August 19, 2016; DOI: 10.1158/0008-5472.CAN-16-0179

proof has been obtained in *Drosophila* where increased symmetric divisions are oncogenic (13, 14). In mammalian systems, however, there is evidence that spindle defects may be both promoting or preventing cancer in different organs (15, 16).

Spindle orientation integrates the action of several multifunctional proteins coordinating the forces between cortex and spindle (17). Among these proteins, RHAMM (also known as HMMR) is of particular interest as it is upregulated in mitosis (18) and localizes at the spindle (19) but is not essential for spindle assembly *in vivo* (20, 21). Nonetheless, spindle orientation fails in female GC follicles (21) and in cultured cells (22) carrying RHAMM truncations. These features make RHAMM a suitable tool in testing whether spindle misorientation can initiate TGCT.

The spindle of dividing rat spermatogonia is preferentially oriented perpendicular to the seminiferous tubule (ST) basal membrane (determining an apicobasal division plane) but when astral microtubules are depolymerized it is reoriented parallel to the basal membrane (planar division; ref. 23). Accordingly, we hypothesized that excessive planar division of undifferentiated spermatogonia promotes their self-renewal and TGCT development.

We used RHAMM mouse transgenesis to test this hypothesis and found that the opposite is true. Impaired planar- and premature apicobasal divisions eliminated or displaced the self-renewing testicular GC from their niche, causing fertility defects, IGCN, and seminoma. We report that the underlying RHAMM spindle function is also abolished in 96% of human seminomas and we determine the molecular cause of this deficiency. We thus identify RHAMM as intrinsic regulator of male GC fate that connects the two clinical pathologies—hypofertility and seminoma.

Materials and Methods

Human testis biopsies

Human testis biopsies were obtained from the Biobank Graz of the Medical University of Graz (MUG, Graz, Austria). The collection and use of the samples were approved by the MUG Ethical Committee.

Mouse transgenesis

The $hmmr^{m/m}$;$Trp53^{-/-}$ mouse was generated by crossing the $hmmr^{m/m}$ (21) with the $Trp53^{-/-}$ line (24).

Cell lines

Flp-In-T-REx-293 cells (Life Technologies) were cultured in DMEM supplemented with 10% tetracycline-free FBS and 2 mmol/L glutamine at 37°C in 5% CO_2. HeLa cells (ATCC CCL-2) were cultured in MEM supplemented with 10% FCS and 2 mmol/L L-glutamine. MEF cells were prepared and cultured as described previously (21). All cell lines were maintained at 37°C in 5% CO_2.

The Flp-In-T-REx-293 and HeLa cell lines were passaged from the commercially obtained master stock four times over 2 weeks, for amplification. The resulting stocks were used in all experiments, for a maximum of 20 passages, with authentication via morphologic and growth criteria specific to each cell line. Further authentication by the suppliers included STR analysis, morphology, and growth assays. The generated Flp-In-T-REx-293 and MEF cell lines were additionally authenticated by PRC using insert/truncation-specific primers (see Supplementary Materials and Methods) and by immunoblotting.

Fertility assays

Mating of 8- to 12-week-old mice was used in the quantification of litter size of homozygous (n1 = 7 mating pairs, n2 = 12 litters, n3 = 46 offspring) or heterozygous (n1 = 14, n2 = 33, n3 = 219) RHAMM-mutant pairs and wild-type controls (n1 = 6, n2 = 6, n3 = 39). Two $hmmr^{m/m}$ male cohorts of different age were used in quantification of litter size, with a minimum of six litters per genotype and age group. In total, 85 litters and 439 offspring were analyzed.

Analysis of GC spindle orientation

Mouse testes were dissected, fixed, and processed according to ref. 21. For analysis of the orientation of spermatogonial cell division plane, testis sections were labeled and imaged as described in the Supplementary Materials and Methods. The angle θ between the cell division plane of (metaphase or anaphase) spermatogonia and the ST basal membrane plane was determined and measured in ImageJ. The long spindle axis, defined as a line across the two centrosomes, was used to determine the cell division plane. The plane of the ST basal membrane, adjacent to the spermatogonium, was defined by a line parallel to the membrane, passing by the membrane/GC contact point.

Histologic analysis, *in situ* hybridization, culture and immortalization of mouse embryonic fibroblasts, preparation of cell protein lysates, SDS-PAGE, and immunoblotting were performed according to ref. 21. RNA interference and high content screening were performed according to refs. 25 and 26 with the modifications described in the Supplementary Materials and Methods.

Statistical analysis

GC spindle orientation was analyzed by the Mann–Whitney test, atrophy, and atypia by the Fisher exact test and all other assays by the two-tailed Student *t* test. Results are presented as mean ± SD, with error bars denoting the SD. The hypothesis that GC spindle orientation is random was tested by the Kolmogorov–Smirnov test.

Results

RHAMM is expressed in male GCs and localizes at their spindle—an association abolished in human testicular GC tumors

Analysis of RHAMM expression and localization in the mouse testis, by radioactive *in situ* hybridization, revealed high transcript levels in a subset of STs (Fig. 1A). This expression pattern is consistent with the organization of spermatogenesis and associated mitoses that occur in "spermatogenic waves" of GC proliferation along the ST epithelium. RHAMM mRNA specifically localized at the outer periphery of the tubules (Fig. 1A), which represent areas of high mitotic activity. Indeed, immunofluorescence microscopy analysis demonstrated RHAMM localization at the mitotic spindle of spermatogonia (Fig. 1B) and spermatocytes (Fig. 1C), which are located at the periphery of the ST.

RHAMM upregulation is commonly observed in cancers, including mammary (27), prostate (28), colorectal (29), hepatocellular (30) carcinomas, and glioblastomas (31), whereas deletion of the RHAMM locus has been reported in malignant

Published OnlineFirst August 19, 2016; DOI: 10.1158/0008-5472.CAN-16-0179

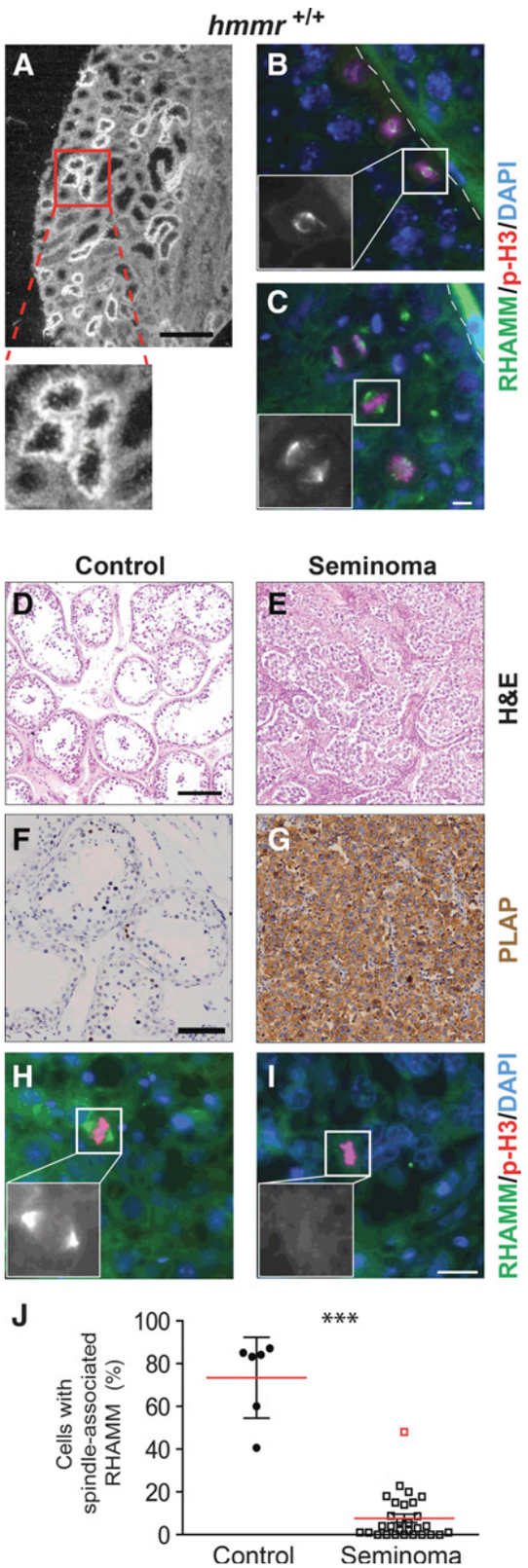

nerve sheath tumors (32). We thus extended the RHAMM expression analysis to 42 human testis biopsy samples (Supplementary Table S1), comprising seminomas ("pure" GC tumors; Fig. 1E) and controls exhibiting no neoplastic lesion (Fig. 1D). Their histopathologic characterization was confirmed by labeling with anti-PLAP antibody (membrane-associated PLacental Alkaline Phosphatase, expressed in GC tumors but not somatic ones; ref. 33; Fig. 1F and G).

RHAMM associated with the mitotic spindle of GCs in control human testes (Fig. 1H), consistent with the protein's localization in cultured cells (Supplementary Fig. S1A; ref. 19) and mouse reproductive organs (Fig. 1A–C; ref. 21). In contrast, spindle-associated RHAMM was undetectable in more than 80% of the metaphase GCs (Fig. 1I and J), in 28 of 29 seminomas analyzed, irrespectively of tumor stage or patient age (Supplementary Table S1). The single tumor exhibiting modest RHAMM spindle localization (indicated in red; Supplementary Table S1 and Fig. 1J) was postsurgically diagnosed as non-Hodgkin lymphoma metastasized to the testis.

These data indicated that RHAMM dissociation from the spindle of GCs is a seminoma-specific phenotype. The very high (96%) prevalence and extremely high significance ($P < 0.001$) of the phenotype suggested RHAMM defects as being central to seminoma, a pathology of largely unknown molecular basis. This prompted us to examine the normal function of RHAMM in the testis and ask whether RHAMM deficiency promotes TGCT development.

The *hmmr*$^{m/m}$ mouse develops several testicular pathologies, including seminoma

RHAMM has two mitotic functions, orienting the spindle (21, 22) and maintaining its integrity (19, 34, 35). Both functions critically depend on the RHAMM C-terminal centrosome-targeting domain, which is necessary for the protein's association with the spindle (19, 21, 34, 35).

To investigate the function of RHAMM in the testis, we used the mouse model *hmmr*$^{m/m}$ carrying a deletion of the C-terminus of the protein (21). A truncated (~65 kDa) RHAMM variant is expressed in the *hmmr*$^{m/m}$ testis (Fig. 2A) and in mouse embryonic fibroblast (MEF$^{m/m}$) cells derived from this line (21). MEFs$^{m/m}$ form mitotic spindles devoid of detectable RHAMM (Supplementary Fig. S1B). The truncated protein carries the N-terminal microtubule-binding RHAMM domain (19), which is functionally

Figure 1.
RHAMM is expressed in male GCs and associates with their spindle; this localization is abolished in human seminoma. Representative sections of wild-type mouse testis (**A–C**), subjected to radioactive *in situ* hybridization, reveals strong expression of RHAMM mRNA in cells along the periphery of STs (**A**). RHAMM localization at the spindle of mouse spermatogonia (**B**) and spermatocytes (**C**) demonstrated by immunofluorescence labeling with anti-RHAMM antibody. Mitotic chromatin and nuclei visualized by anti-pH3 and DAPI labeling. Dashed lines, the ST basal membrane; magnified insets show anti-RHAMM labeling. Sections of human testes from control (**D**, **F**, and **H**) and seminoma (**E**, **G**, and **I**) biopsies stained with hematoxylin and eosin (H&E; **D** and **E**) or anti-PLAP (**F** and **G**) and anti-RHAMM antibodies (**H** and **I**). Additional immunofluorescence labeling and insets as in **B** and **C**. **J,** quantification of testicular mitotic cells with spindle-associated RHAMM in control and seminoma human biopsies. Red square, biopsy postsurgically diagnosed as testicular metastasis of non-Hodgkin lymphoma). $n = 100$ metaphase cells/sample; ***, $P < 0.001$. Scale bars, 1 mm (**A**), 10 μm (**B** and **C**), 100 μm (**D** and **F**), and 20 μm (**H** and **I**).

Published OnlineFirst August 19, 2016; DOI: 10.1158/0008-5472.CAN-16-0179

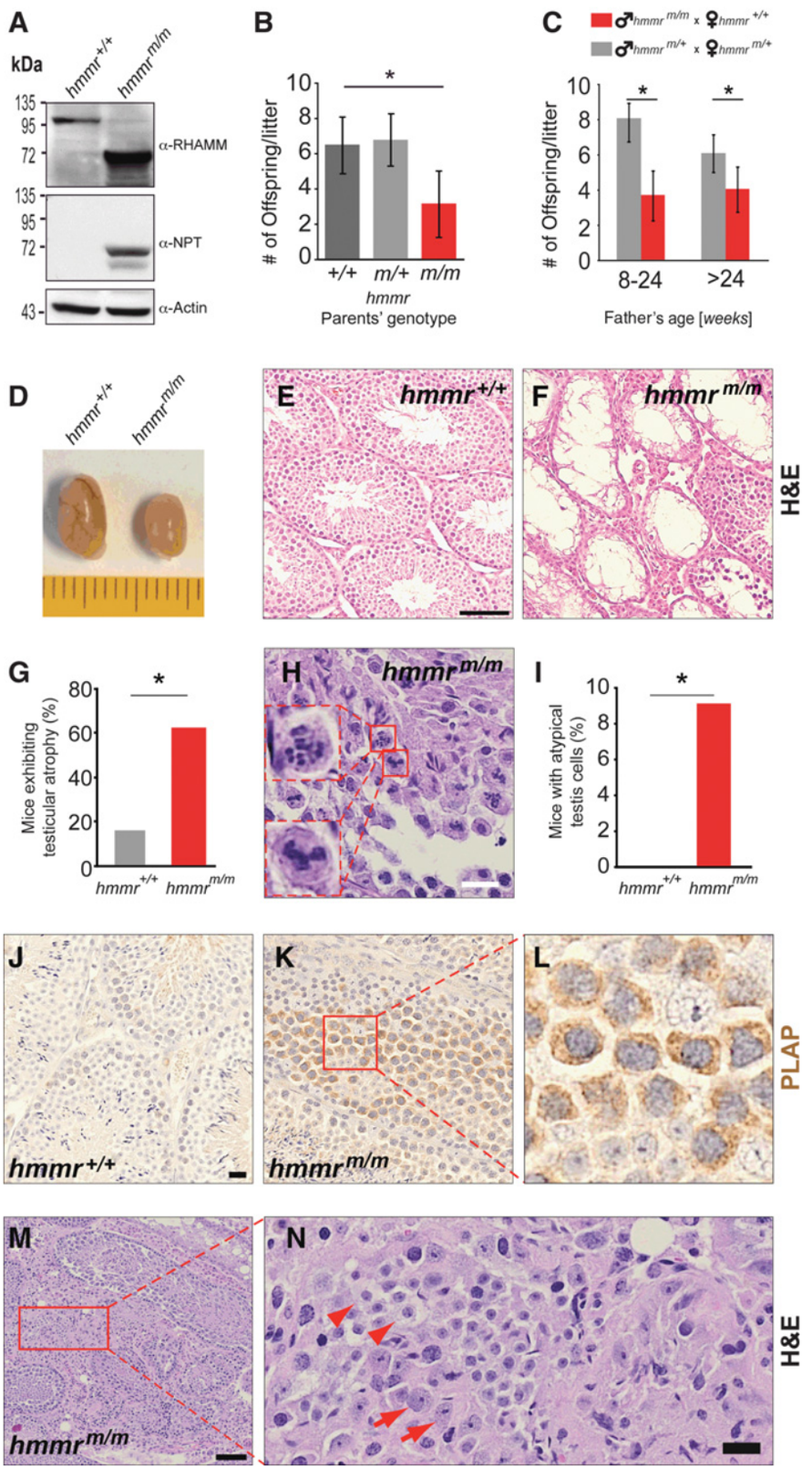

Figure 2.

Elimination of the RHAMM centrosome-targeting domain causes testicular atrophy, hypofertility, and seminoma development. **A,** full-length (95 kDa) RHAMM expressed in $hmmr^{+/+}$ testis; $hmmr^{m/m}$ counterparts express a truncated 65-kDa protein fused to NPT. Western blot analysis probed with the indicated antibodies. Loading control, β-actin. **B** and **C,** litter size (denoted by average number of offspring/litter) produced by mating pairs of the indicated genotypes more than 6 months. Mating pairs in **B:** $+/+$ $n = 6$, m/+ $n = 14$, m/m $n = 7$; in **C:** 8 to 24 week-old, m/+ $n = 6$, m/m $n = 4$; >24 week-old, m/+ $n = 7$, m/m $n = 6$. Testes of 6-week-old mice, prepared for gross examination, demonstrate testicular atrophy affecting $hmmr^{m/m}$ (**D**), confirmed by hematoxylin and eosin (H&E) staining (**E** and **F**) and quantification (**G**). $hmmr^{+/+}$, $n = 63$; $hmmr^{m/m}$, $n = 77$ animals. Atypical GCs in the ST lumen of $hmmr^{m/m}$ testes visualized by H&E staining (**H**) and quantified (**I**; *n* numbers as in **G**). **J–L,** increased PLAP expression in $hmmr^{m/m}$ testis indicates IGCN. IHC labeling of one-year-old mouse testes with anti-PLAP antibody. **M** and **N,** seminoma in H&E–stained $hmmr^{m/m}$ testis section. Seminoma cells with enlarged nuclei (arrow) and clear cytoplasm (arrowhead) are indicated (**N**). *, $P < 0.05$. Scale bars, 100 μm (**E**, **F**, and **M**) and 20 μm (**H**, **J**, **K**, **L**, and **N**).

Published OnlineFirst August 19, 2016; DOI: 10.1158/0008-5472.CAN-16-0179

intact, as indicated by its association with microtubules when overexpressed (Supplementary Fig. S2).

Homozygous *hmmr*$^{m/m}$ mouse matings yielded significantly decreased litter size, compared with wild-type *hmmr*$^{+/+}$ controls, indicating fertility defects (Fig. 2B). To distinguish male fertility defects from the previously reported maternal hypofertility of this line (21), the *hmmr*$^{m/m}$ males were mated with wild-type females (Fig. 2C). These males were severely hypofertile, as indicated by the decreased litter size independently of the father's age (Fig. 2C).

RHAMM was reported to regulate human sperm motility (36). However, analysis of several spermatozoa motility parameters showed no motility differences among sperm isolated from the epididymis of *hmmr*$^{m/m}$ *versus* *hmmr*$^{+/+}$ males (Supplementary Fig. S3A). This finding suggests that RHAMM centrosomal functions are not required for sperm motility and that the observed *hmmr*$^{m/m}$ hypofertility had other causes.

Gross examination revealed reduced size of the *hmmr*$^{m/m}$ testes (Fig. 2D), consistent with severe atrophy of the STs (Fig. 2F), which is histopathologically apparent from 5 weeks of age. In *hmmr*$^{+/+}$ testes, GCs in different stages of differentiation as well as Sertoli cells were observed within ST of normal appearance (Fig. 2E), whereas the testes of *hmmr*$^{m/m}$ littermates displayed STs with markedly depleted GCs or completely degenerated STs devoid of GC and sperm cells (Fig. 2F), indicating defective spermatogenesis. Atrophy was observed in 62% of *hmmr*$^{m/m}$ versus 16% of *hmmr*$^{+/+}$ mice (Fig. 2G). Neither tubular sclerosis nor interstitial fibrosis between STs could be detected, indicating that the GC aplasia is not the result of chronic inflammation.

In a significant number of RHAMM-mutant males (9.1% *hmmr*$^{m/m}$, 0% *hmmr*$^{+/+}$) older than 30 weeks of age, the ST lumen contained high numbers of atypical GCs (Fig. 2H and I). These cells displayed abnormal mitosis or apoptotic nuclear fragmentation (Fig. 2H), a pathology resembling IGCN, the precursor lesion of seminoma. Indeed, cells labeled with anti-PLAP, a marker of IGCN (37) and seminoma (33), were localized within the adluminal area of the STs in *hmmr*$^{m/m}$ testes (Fig. 2K and L), suggesting that the atypical cells are seminoma precursors. In a cohort of males (follow-up until end of life is ongoing), seminoma occurred in 3.7% of *hmmr*$^{m/m}$ (0% of *hmmr*$^{+/+}$), characterized by GCs with enlarged nuclei and clear cytoplasm as well as invasive tumor growth into the neighboring interstitial tissue (Fig. 2M and N).

In summary, the *hmmr*$^{m/m}$ male mice exhibit an early-onset testicular atrophy, hypofertility, cellular atypia, and seminoma. The *hmmr*$^{m/m}$ males phenocopy the human pathology (2, 3) and are thus suited in elucidating the pathophysiologic function of RHAMM in the etiology of hypofertility and TGCT.

Elimination of the RHAMM centrosomal function promotes p53-dependent GC apoptosis

A 3-fold increase in apoptotic GCs was observed in *hmmr*$^{m/m}$ testes, already at a very young age (Fig. 3A–C). The high incidence of testicular atrophy and the low incidence of seminoma suggested that activation of tumor suppression pathways may be responsible for the elimination of atypical cells, preventing development of the seminoma precursor lesion, albeit at the cost of atrophy and hypofertility.

Accordingly, expression of the p53 protein, a canonical tumor suppressor, was elevated in *hmmr*$^{m/m}$ testes (Fig. 3D). Constitutive activation of p53 in the testis causes GC apoptosis, thereby leading to testicular atrophy (38). To test whether p53 activation is responsible for the GC depletion and seminoma suppression in *hmmr*$^{m/m}$, we crossed these mice with the *Trp53*$^{-/-}$-mutant line (24). The p53 deletion did not affect RHAMM expression in the testis (Fig. 3E).

As expected, ablation of p53 rescued the GC apoptosis in *hmmr*$^{m/m}$ testes (Fig. 3C). However, the testicular atrophy persisted in 30% of *hmmr*$^{m/m}$;*Trp53*$^{-/-}$ (Fig. 3G and H), indicating a more complex etiology underlying this phenotype. In addition, GC apoptosis affected animals as young as 4-week old (Fig. 3C), whereas atypia appeared from circa 30 weeks of age, suggesting that apoptosis and atypia are not related.

Mitotic delays induce p53 upregulation and apoptosis (39). Could the RHAMM truncation cause such mitotic delay? MEFs$^{m/m}$, in contrast to MEFs$^{+/+}$, formed spindles devoid of RHAMM (Supplementary Fig. S1B), exhibited a 2-fold increase in spindle assembly defects but progressed through the cell cycle without significant delay (Supplementary Fig. S1C). The highest p53 expression was observed in spermatogonia of the *hmmr*$^{m/m}$ (Fig. 3J), suggestive of mitotic defects or mitotic delays in these cells brought about by the RHAMM truncation. One could hypothesize that such cells are eliminated from the stem cell pool (39). However, no spindle abnormalities were observed in hundreds of spermatogonia analyzed (Figs. 3K and L and 4), suggesting that RHAMM is dispensable for bipolar spindle assembly *in vivo*, in agreement with previous studies (20, 21).

In conclusion, the ST atrophy and hypofertility cannot be explained solely by spindle assembly defects or delays and p53-dependent apoptosis, as removal of p53 only partially relieves the (atrophy) phenotype. These data suggest that another function of RHAMM must be impaired in the *hmmr*$^{m/m}$ males. We thus asked whether spindle orientation (a RHAMM C-terminus function) is pertinent to spermatogenesis and TGCT development.

RHAMM regulates the oriented division of male GCs

RHAMM localization at the spindle of spermatogonial (Fig. 1B, 4A) and spermatocytic (Fig. 1C, 4C) GCs is abolished in *hmmr*$^{m/m}$ (Fig. 4B and D). This is in agreement with *in vitro* (Supplementary Fig. S1B; ref. 34) and *in vivo* (21) data showing the RHAMM centrosome-targeting domain to be necessary for association of the protein with the spindle. Given its dispensable role in spindle assembly *in vivo*, we subsequently explored whether RHAMM is required for spindle orientation during spermatogenesis.

Spermatogonial but not spermatocytic divisions are oriented in the rat testis (23). We thus analyzed spermatogonial spindle orientation, in 5- to 10-week-old *hmmr*$^{m/m}$ and control mice. For each metaphase spermatogonium, the angle θ, defined by the cell division plane and the ST basal membrane plane, was measured (Fig. 4E and I, see also Materials and Methods). Testes harbor undifferentiated and differentiating spermatogonia (9). The former express PLZF and the latter β-catenin, in mutually exclusive manner (Supplementary Fig. S3D). Of note, in addition to its nuclear expression, β-catenin localized at the apical surface of differentiating spermatogonia, suggesting a polarity function of the protein (Supplementary Fig. S3E).

In wild-type testes, the small θ (median 6.2°) of PLZF-positive spermatogonia indicates that they orient their spindle parallel to the basal membrane of the seminiferous epithelium, suggesting that undifferentiated spermatogonia undergo planar cell division

Published OnlineFirst August 19, 2016; DOI: 10.1158/0008-5472.CAN-16-0179

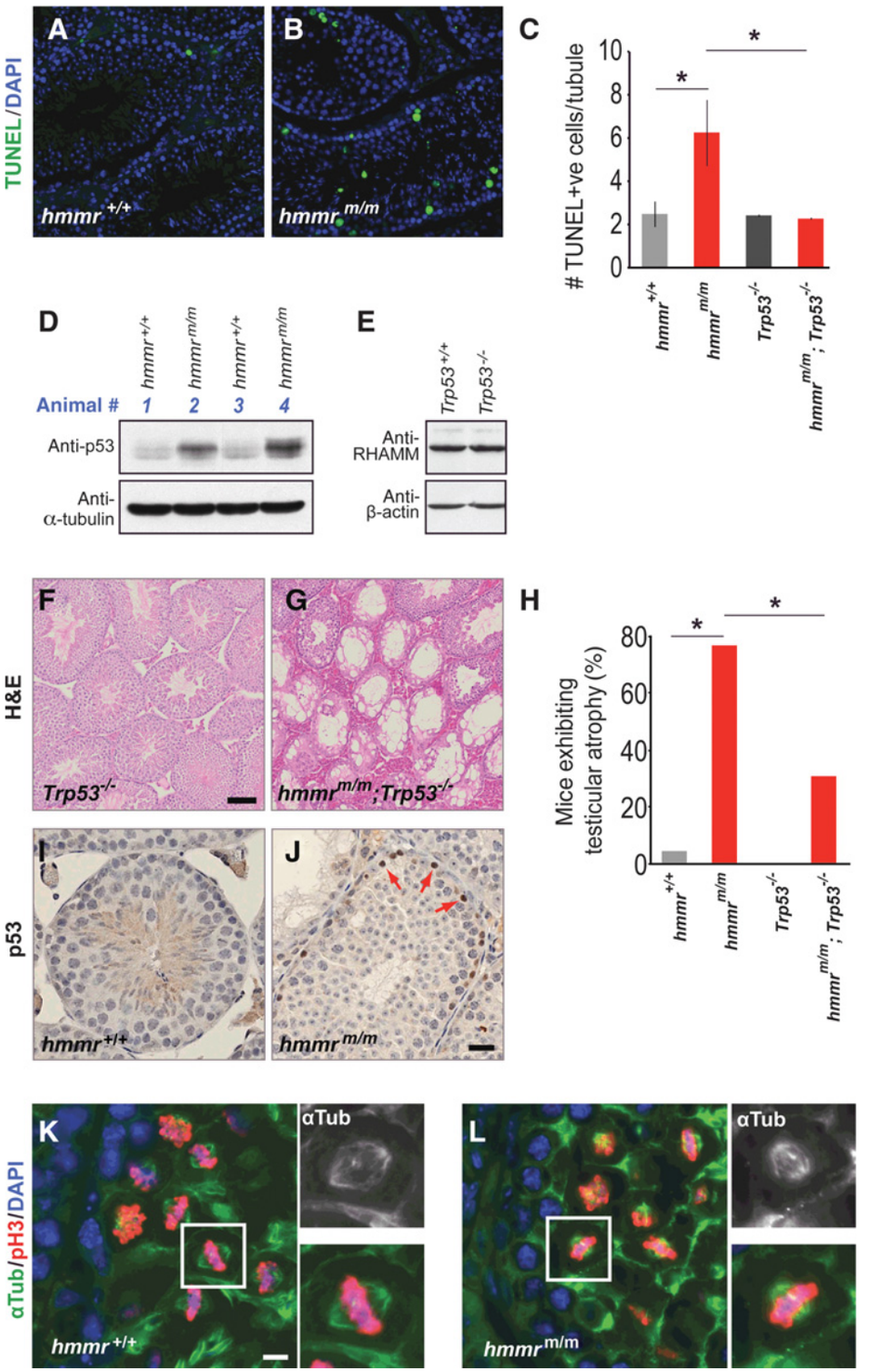

Figure 3.

Elimination of the RHAMM centrosome-targeting domain causes p53-dependent GC apoptosis. **A–C,** GC apoptosis in testes of 5- to 10-week-old animals of the indicated genotypes, demonstrated by TUNEL labeling. Quantification in **C**. $hmmr^{+/+}$, $n = 3$; $hmmr^{m/m}$, $n = 3$; $Trp53^{-/-}$, $n = 2$; $hmmr^{m/m}$; $Trp53^{-/-}$, $n = 3$ animals. **D** and **E,** upregulation of p53 in $hmmr^{m/m}$ testis. RHAMM protein expression in $Trp53^{-/-}$ testis is unaffected by the p53 deletion. Western blots (**D** and **E**) probed with the indicated antibodies. Loading controls, α-tubulin/β-actin. **F–H,** p53 deletion fails to rescue the ST atrophy of $hmmr^{m/m}$. Hematoxylin and eosin (H&E)–stained testis sections from 6-week-old males of the indicated genotypes. Quantification in **H**. $hmmr^{+/+}$, $n = 23$; $hmmr^{m/m}$, $n = 30$; $Trp53^{-/-}$, $n = 5$; $hmmr^{m/m}$; $Trp53^{-/-}$, $n = 13$ animals. **I** and **J,** elevated p53 protein expression in $hmmr^{m/m}$ spermatogonia (arrows), demonstrated by IHC labeling. No spindle assembly defects were observed in $hmmr^{m/m}$ spermatocyte (**L**) or controls (**K**). Immunofluorescence labeling with the indicated antibodies. *, $P < 0.05$. Scale bars, 100 μm (**A**, **B**, **F**, **G**), 20 μm (**I** and **J**) and 10 μm (**K** and **L**).

(Fig. 4F). In contrast, the average θ angle in the $hmmr^{m/m}$ testes was significantly higher (median $\theta = 32.1°$), due to a wider distribution of this parameter (Fig. 4G). The $hmmr^{m/m}$ data set included spindles positioned perpendicular to the ST membrane. The distribution of spindle angles in the mutant PLZF-positive spermatogonia did not differ from the random distribution (Kolomogorov–Smirnov test, $P = 0.099$), contrary to $hmmr^{+/+}$ where spindle angles differed very significantly ($P < 2.2 \times 10^{-16}$) from the random distribution (Fig. 4H).

In contrast to undifferentiated GCs, the high θ (median 63.7°) of differentiating β-catenin–positive spermatogonia in wild-type testis indicates that they orient their spindle perpendicular to the

Published OnlineFirst August 19, 2016; DOI: 10.1158/0008-5472.CAN-16-0179

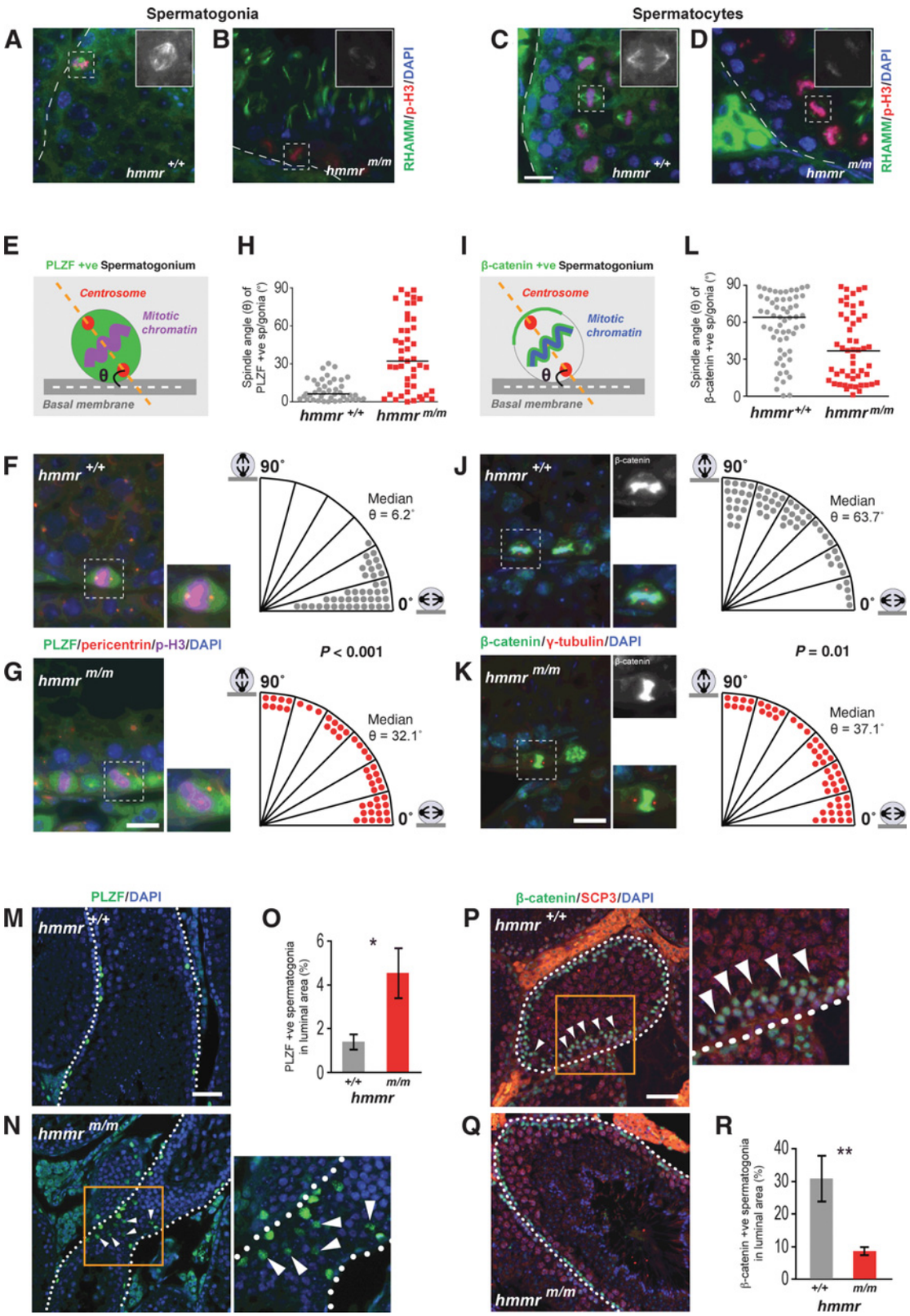

Published OnlineFirst August 19, 2016; DOI: 10.1158/0008-5472.CAN-16-0179

ST basal membrane, generating apical and basal daughter cells (Fig. 4J). In $hmmr^{m/m}$, the average θ angle was significantly lower (median 37.1°; Fig. 4K). The $hmmr^{+/+}$ β-catenin–positive spermatogonia exhibited preferential spindle orientation ($P = 0.0011$ vs. random distribution) and this preference was impaired in their $hmmr^{m/m}$ counterparts ($P = 0.0477$; Fig. 4L).

These data suggest that spermatogonial stem cells undergo planar division and reinforce the notion that the activity of RHAMM, via its centrosome-targeting domain, is essential for these stereotypical divisions in the testis. The random spindle positioning in $hmmr^{m/m}$ spermatogonia most probably contributes to alterations in the geometry of planar divisions of undifferentiated GCs. These divisions are critical for GC renewal and a functional testis.

Further to the GC depletion, the symmetric segregation of PLZF during anaphase, which is independent of spindle orientation (Supplementary Fig. S3F and S3G), indicated that displacement of the GCs from the basal compartment can be analyzed using differentiation cell markers. This analysis demonstrated premature displacement of undifferentiated spermatogonia from the niche in $hmmr^{m/m}$ (Fig. 4M–O), whereas the translocation of differentiated spermatogonia into the ST lumen was prevented (Fig. 4P–R).

Spindle orientation entails RHAMM-mediated recruitment of CHICA and DYNLL1 (component of the dynein motor complex) to the spindle (22). In agreement with the impairment of spindle orientation in the mutant testis, the C-terminus truncation of RHAMM (expressed in $hmmr^{m/m}$) prevents formation of the RHAMM–CHICA–DYNLL1 tripartite complex (Fig. 5).

Combined with the phenotypic analysis of $hmmr^{m/m}$ males, the above data suggest that impaired orientation of GC division contributes to two distinct phenotypes that occur at different frequencies: The most prevalent is GC depletion with consequent testicular atrophy and hypofertility. The second phenotype comprises premature localization of undifferentiated GCs outside the basal compartment, cellular atypia, IGCN, and seminoma.

As RHAMM dissociation from the spindle of GCs appears to be critical in the etiology of the $hmmr^{m/m}$testicular phenotypes and it is highly prevalent (96%) in human seminoma (Fig. 1H–J), we investigated the underlying molecular mechanism.

RHAMM variants do not affect the protein's spindle localization

TGCT exhibit deletions and re-arrangements in the human locus *5q34*, where RHAMM is encoded (40). We thus postulated that RHAMM spindle mislocalization in seminoma (Fig. 1) is due to RHAMM genomic defects. Targeted sequencing of the *Hmmr* locus in the human biopsies and investigation of the allele frequencies detected allelic imbalance, which might indicate LOH, in 12% of seminoma samples (Supplementary Table S1). In addition, six missense variants in the RHAMM protein-coding region were identified. They were compared with their frequency in the population using data from the 1000 Genomes Project, while their impact on protein structure was evaluated using PolyPhen (Supplementary Table S1 and Fig. 6A and B).

We assessed the functional significance of the missense variants for spindle localization of RHAMM in cultured human cells. RHAMM encodes a microtubule-binding domain (Fig. 6A) that, upon overexpression, stabilizes microtubules, leading to cell-cycle arrest. This was prevented by inducible expression of the variants at low level (Fig. 6C), in cells treated with siRNA targeting the 3′UTR of RHAMM, to silence endogenous RHAMM expression. The two most common variants (V368A, A484V) were tested in tandem as they appear in tandem in the biopsies (Supplementary Table S1). They did not affect RHAMM spindle localization, but neither did the remaining four variants (tested in the presence of V368A and A484V; Fig. 6C).

In conclusion, the RHAMM mislocalization in human seminoma could not be attributed to its functional inactivation.

RHAMM mRNA is downregulated in human seminoma

However, we found extremely significant downregulation of RHAMM mRNA expression in the seminoma biopsies (Fig. 6D and Supplementary Table S1). As RHAMM expression peaks at G_2–M (18), it positively correlated with expression of the mitotic cyclin B1 (Fig. 6F, $r = 0.828$). Even normalized against cyclin B1 levels (to account for putative differences in the mitotic index), the downregulation of RHAMM mRNA in seminoma remained very significant (Fig. 6E).

Although the molecular basis of seminoma development remains unknown, GWAS have identified 12 TGCT susceptibility genes (4–7). In the biopsies, two of the genes (*ATF7IP* and *MAD1L1*) exhibit differential mRNA expression (control vs. seminoma) but neither has known spindle-associated functions (Supplementary Fig. S4A).

We conclude that, in human seminoma, delocalization of RHAMM from the mitotic spindle is likely caused by decreased RHAMM expression but not due to mutations or deletions in the *Hmmr* locus. We thus sought to identify regulators of RHAMM expression.

Figure 4.

Dissociation of RHAMM from the spermatogonium spindle results in its misorientation and the localization of undifferentiated GCs at the ST lumen. **A–D,** RHAMM spindle localization in $hmmr^{+/+}$ spermatogonia (**A**) and spermatocytes (**C**) is eliminated in their $hmmr^{m/m}$ counterparts (**B** and **D**). Immunofluorescence labeling of mouse testis sections with the indicated antibodies. Dashed line, the ST basal membrane; magnified insets show anti-RHAMM labeling. Schematic illustration of the spindle orientation assay applied to undifferentiated (**E**) and differentiating (**I**) spermatogonia. Detailed description under Materials and Methods. Small θ indicates planar and large θ apicobasal division (cartoons in **F**, **G**, **J**, and **K**). Undifferentiated PLZF-expressing spermatogonia orient their spindle axis parallel to the ST basal membrane, as indicated by the small θ (median 6.2°; **F**). The division orientation is randomized in $hmmr^{m/m}$ spermatogonia (median $\theta = 32.1°$; **G**), which assemble bipolar spindles devoid of RHAMM (**B**). Differentiating β-catenin–expressing spermatogonia orient their spindle axis perpendicular to the ST basal membrane, as indicated by the large θ (median $\theta = 63.7°$; **J**). The division orientation is randomized in $hmmr^{m/m}$ spermatogonia (median $\theta = 37.1°$; **K**). Further statistical analysis in Supplementary Materials and Methods. Every dot in the quadrants (**F**, **G**, **J**, and **K**) and dot plots (**H** and **L**) represents one mitotic spermatogonium; line indicates median θ (**H** and **L**). The localization of undifferentiated spermatogonia (PLZF+ve) adjacent to the ST basal membrane (**M**) is compromised in $hmmr^{m/m}$ testes, which present undifferentiated GC in the lumen (**N**, arrowheads; **O**). Conversely, the number of differentiating spermatogonia (β-catenin+ve and SCP3−ve) localized apically of the ST basal membrane (**P**, arrowheads) is reduced in $hmmr^{m/m}$ testes (**Q** and **R**). Immunofluorescence labeling with the indicated antibodies. SPC3 labeling distinguishes lumen-localized differentiating spermatogonia from spermatocytes (which express SCP3 and localize in the lumen); $n = 3$ males/genotype. *, $P < 0.05$; **, $P < 0.01$. Scale bars, 50 μm (**M** and **P**) and 20 μm (**A–D**, **G**, and **K**).

Published OnlineFirst August 19, 2016; DOI: 10.1158/0008-5472.CAN-16-0179

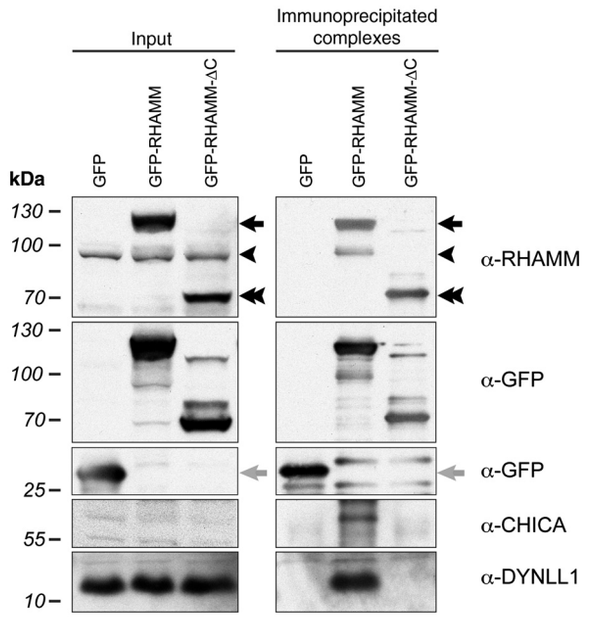

Figure 5.

Truncation of the RHAMM C-terminus (RHAMM-ΔC) abolishes the protein's association with CHICA and DYNLL1. Expression and immunoprecipitation (via anti-GFP) of the indicated proteins is demonstrated by Western blot analysis. GFP-RHAMM (arrow), endogenous RHAMM (arrowhead), GFP-RHAMM-ΔC (double arrowhead), GFP (gray arrow).

CFIm25 regulates RHAMM expression

To identify RHAMM regulators, we developed an immunofluorescence-based RNAi screening assay (outlined in Supplementary Fig. S5A) for the identification of mitotic cells and the quantitative analysis of spindle-associated RHAMM by high-content screening microscopy (25, 26). We screened a custom library of 1,634 genes, including the 12 TGCT susceptibility genes as well as genes encoding centrosome/spindle-associated factors and their regulators. The library and the analysis criteria applied for hit identification are described in the Supplementary Materials and Methods.

The primary screen identified 26 positive RHAMM regulators. Among the top scoring hits was CFIm25 (also known as NUDT21 or CPSF5), knockdown of which resulted in 2-fold decrease of spindle-associated RHAMM (Supplementary Fig. S5B). From the TGCT susceptibility genes, six were identified as negative RHAMM regulators, as their silencing significantly increased spindle-associated RHAMM (Supplementary Fig. S5B). However, knockdown of ATF7IP and MAD1L1 (which were downregulated in the seminomas; Supplementary Fig. S4A) resulted in elevated RHAMM level (ATF7IP) or had no effect (MAD1L1; Supplementary Fig. S5B). Validation of selected hits is shown in Supplementary Fig. S5C to S5E.

CFIm25 is a core component of the mRNA Cleavage Factor I [CFIm, also known as cleavage and polyadenylation specificity factor (CPSF)] that functions in alternative polyadenylation (APA). This process modulates gene expression by regulating the length of mRNA 3′UTR impacting mRNA stability (41). CFIm components are highly expressed in the testis (42). We thus investigated further the role of CFIm25 in RHAMM regulation.

The siCFIm25-treated cells exhibit 60% RHAMM mRNA decrease (Fig. 7A and B), suggesting that reduction of RHAMM mRNA by silencing CFIm25 was responsible for the significant downregulation of the RHAMM protein, detected in the RNAi screen. Immunoblotting and immunofluorescence microscopy analysis of siCFIm25-treated cells confirmed the downregulation of total (Fig. 7C) and spindle-associated (Fig. 7D) RHAMM protein.

We conclude that CFIm25 positively regulates RHAMM mRNA stability and consequently RHAMM expression.

CFIm25 expression is downregulated in human seminoma

Consistent with its role in RHAMM regulation, CFIm25 mRNA was significantly downregulated in the seminomas (Supplementary Table S1; Fig. 7E). At the protein level (analyzed in sections of the FFPE biopsies), CFIm25 was undetectable in the nuclei of seminoma cells (Fig. 7G) whereas strongly expressed in nuclei of spermatogonial and spermatocytic nuclei of control testes (Fig. 7F; ref. 42).

In addition to RHAMM, two TGCT susceptibility genes (ATF7IP and MAD1L1) were downregulated in the seminomas (Supplementary Fig. S4A). However, in the cellular system, neither was modulated by CFIm25 knockdown (Supplementary Fig. S4B). These data reinforce the notion that the activity of CFIm25 specifically regulates RHAMM expression in the testis.

We conclude that impaired CFIm25 expression and consequent RHAMM downregulation disrupt planar cell division of undifferentiated GCs, generating two clinically linked phenotypes: (i) testicular atrophy and hypofertility, likely caused by depletion of the GCs from the seminiferous epithelium niche; (ii) cellular atypia, intratubular GC neoplasias and seminoma, attributed to the premature displacement of undifferentiated GCs from the ST basal compartment.

Discussion

RHAMM defects provide a common etiology of hypofertility and seminoma

Human TGCTs are cancers of GC lineage, clinically linked to testicular GC depletion—a pathology primarily manifested by hypo/infertility (3), preceeding TGCT development. Therefore, a unifying mechanism of TGCT oncogenesis should provide a comprehensive explanation for both hypofertility and tumorigenesis. We show that RHAMM defects generate both phenotypes in the same murine $hmmr^{m/m}$ individuals: testicular atrophy and hypofertility of early onset, followed by IGCN and seminoma. Thus, our data reveal RHAMM defects as the common molecular etiology underlying the two clinically linked pathologies.

RHAMM downregulation and delocalization from the spindle appear central to seminoma development

The notion that RHAMM has a central role in TGCT etiology is reinforced by three additional datasets. Human RHAMM is encoded in locus *5q34*. Loss of heterozygosity and allelic imbalance studies of TGCT have identified deletions and rearrangements in *5q34* (40), which has been suggested to bear a candidate TGCT suppressor (43).

Second, we show that, in human seminoma, RHAMM mRNA downregulation and protein dissociation from the spindle occur at extremely high prevalence (96% for the latter) and significance ($P < 0.001$ for both). In comparison, activating KIT mutations

Published OnlineFirst August 19, 2016; DOI: 10.1158/0008-5472.CAN-16-0179

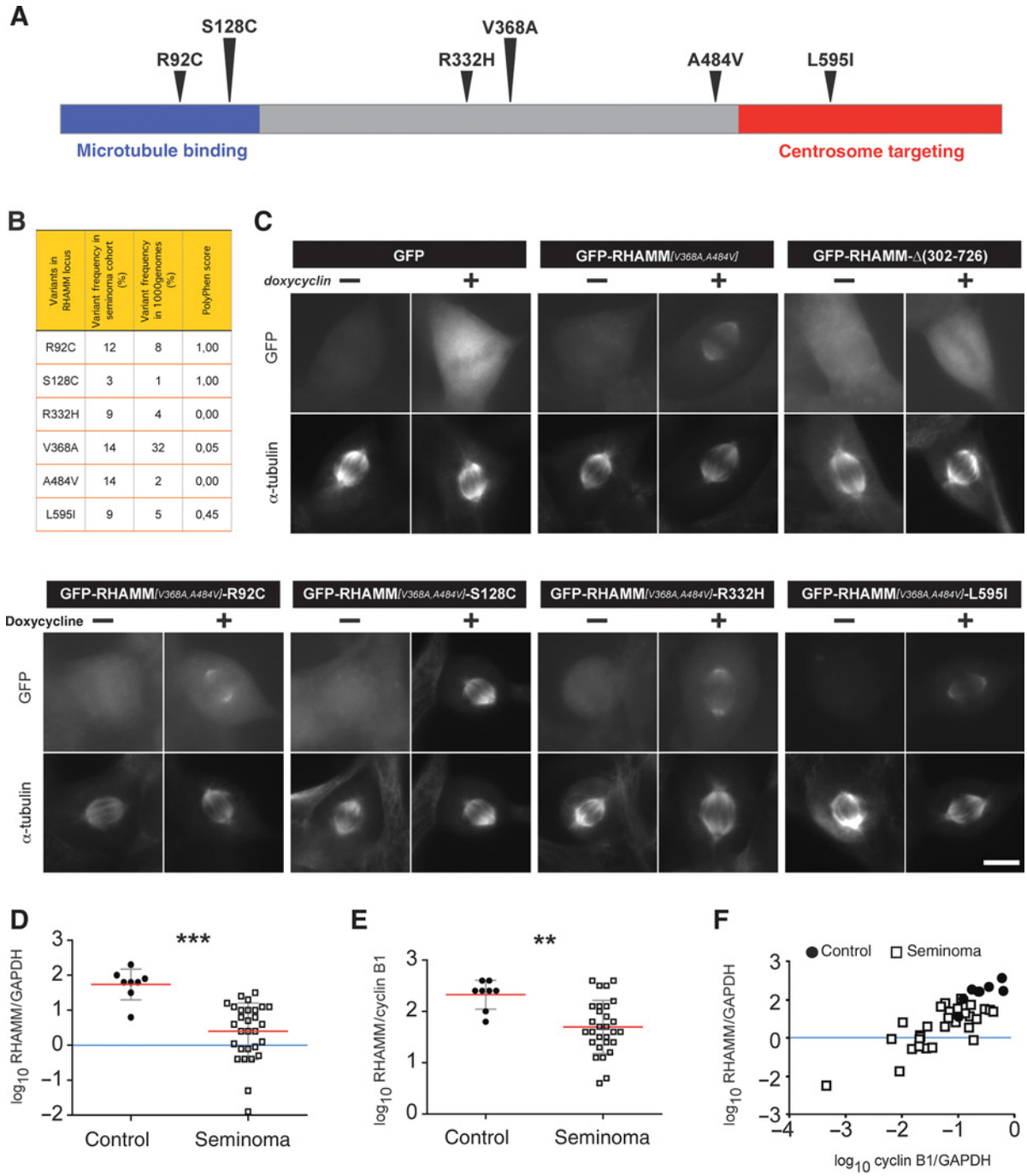

Variants in RHAMM locus	Variant frequency in seminoma cohort (%)	Variant frequency in 1000genomes (%)	PolyPhen score
R92C	12	8	1,00
S128C	3	1	1,00
R332H	9	4	0,00
V368A	14	32	0,05
A484V	14	2	0,00
L595I	9	5	0,45

Figure 6.

RHAMM variants and RHAMM mRNA downregulation in human seminoma. **A,** schematic representation of the RHAMM protein indicating the microtubule binding & centrosome targeting domains and the missense variants identified in human testes biopsies. **B,** frequency of RHAMM variants, identified in human testes, and PolyPhen score. See also Supplementary Table S1. **C,** all (GFP-tagged) RHAMM variants localized at the spindle, as demonstrated by the GFP signal (expression induced by doxycyclin). Spindle microtubules were counter-labeled with anti-α-tubulin. Truncated RHAMM-Δ(302-726) and GFP used as negative controls. Scale bar, 10 μm. Extremely significant reduction of RHAMM mRNA [normalized to GAPDH (**D**) or cyclin B1 (**E**)] in 29 seminoma biopsies. RHAMM expression correlated positively with cyclin B1 expression (**F**). ***, $P < 0.0001$ ($P = 0.0000027$); **, $P < 0.01$ ($P = 0.0024$).

appear in approximately 20% of seminomas (1), whereas multiple GWAS-identified loci associated with TGCT account altogether for approximately 25% to 32% of the genetic risk of developing TGCT (4, 5). In this context, the ubiquitous occurrence of the RHAMM defect raises the possibility that RHAMM represents a convergence hub of the activity of multiple TGCT

Published OnlineFirst August 19, 2016; DOI: 10.1158/0008-5472.CAN-16-0179

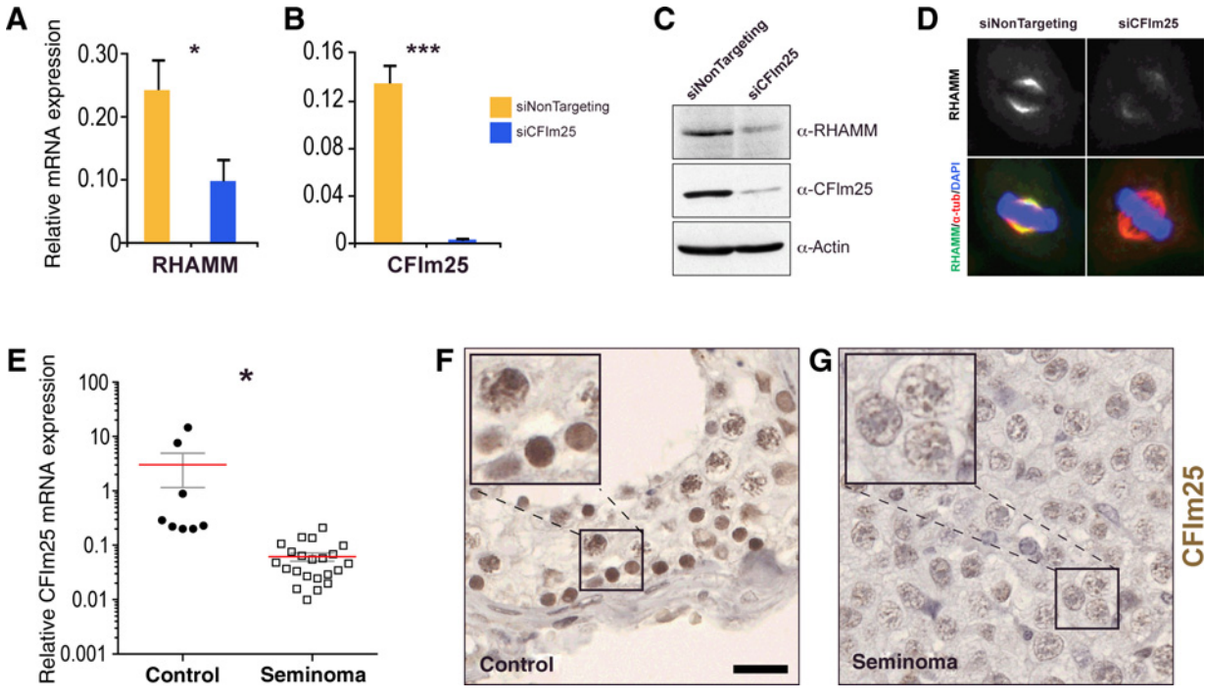

Figure 7.

CFIm25 positively regulates RHAMM mRNA expression. siRNA-mediated CFIm25 knockdown significantly reduces RHAMM mRNA (**A**) and protein (**C**) expression, eliminating RHAMM spindle localization (**D**). siCFIm25 silencing efficiency indicated by CFIm25 mRNA level in the same cells (**B**). *, $P < 0.05$ ($P = 0.016$); ***, $P < 0.001$ ($P = 0.00011$). **C,** Western blot probed with the indicated antibodies. Loading control, β-actin. **D,** HeLa cells, immunofluorescence-labeled with the indicated antibodies; scale bar, 10 μm. **E,** CFIm25 mRNA expression (normalized to GAPDH) is significantly reduced in human seminoma. *, $P < 0.05$ ($P = 0.012$). **G** and **F,** IHC labeling demonstrates the CFIm25 protein downregulation in human seminoma (**G**), compared with control testis (**F**). Scale bar, 20 μm.

susceptibility genes or loci. In support of this hypothesis, we show that expression changes in TGCT susceptibility genes, in human cells, significantly modulate RHAMM levels.

Third, we show RHAMM expression and localization to be positively regulated by CFIm25, a testis-specific protein (42) significantly and consistently downregulated in the seminomas. CFIm25 forms a heterotetramer with CFIm68, which preferentially binds the UGUA sequence of mRNA, thereby recruiting components for the cleavage and polyadenylation of the proximal (rather than distal) mRNA 3′-end. Many testis-specific genes preferentially employ proximal mRNA polyadenylation (42), suggesting that the high testicular CFIm25 levels reflect and promote this type of regulation. Besides its postulated function in spermatogenesis, a role for APA in oncogenesis is emerging (44).

The orientation of spermatogonial divisions is stereotyped and depends on the CG differentiation stage

The spindle acts as mitotic spatial regulator in female gametogenesis (45, 21). We now demonstrate its role in spermatogenesis, where orientation of the GC division plane depends on the differentiation stage of these cells. The planar division of undifferentiated spermatogonia likely reflects self-renewal/trans-amplification of undifferentiated cells, supported by the symmetric segregation of PLZF (Supplementary Fig. S3F and S3G). Nonetheless, the existence of other spermatogonial markers that segregate asymmetrically in these GCs cannot be excluded (46). In contrast, apicobasal division signals transition from self-renewal/trans-amplification to differentiation. This transition could be attributed to the apical surface localization of β-catenin, revealed by our analysis. During heart development, β-catenin is essential in establishing cell polarity for epicardial spindle orientation (47). It is probable that β-catenin functions in a similar manner to direct GC differentiation.

Disruption of oriented division leads to depletion of GCs, testicular atrophy, and hypofertility

Spindle-associated RHAMM is essential for oriented division during spermatogenesis. GC spindles devoid of RHAMM are randomly oriented, but how could this misorientation result in GC depletion? On the basis of our data, at least two possibilities can be envisioned: defects in tissue homeostasis due to depletion of undifferentiated GCs and/or defects in differentiation.

For undifferentiated spermatogonia, the basal compartment of the ST epithelium, functioning as niche, provides signals for the self-renewal of the stem cell population (48). We propose that the increased apicobasal division of $hmmr^{m/m}$ undifferentiated spermatogonia disrupts stem cell homeostasis, by altering the spatiotemporal placement of undifferentiated progenies, thereby leading to loss of self-renewal signals from the niche. In support of this notion, spindle orientation dictates the cell fates of, for example, brain (12) or hematopoietic (16) stem cell populations, with negative consequences for tissue homeostasis when disrupted. The RHAMM-dependent apicobasal division of differentiating spermatogonia is consistent with the apical progression of spermatogenesis in the ST, via successive apicobasal divisions (9). As differentiating spermatogonia enter differentiation in a

Published OnlineFirst August 19, 2016; DOI: 10.1158/0008-5472.CAN-16-0179

synchronized manner (9), it is plausible that random division orientation impairs this synchronization in *hmmr*$^{m/m}$, resulting in decreased number of GCs committed to differentiation. The two defects likely converge to cause GC depletion.

Could p53 function in GC depletion? The persistence of ST atrophy in p53-null background suggests that the consequences of spindle misalignment do not involve p53. If at all involved, evidence that p53-null stem cells switch from asymmetric to self-renewing divisions (49) raises the possibility that p53 deletion enhances self-renewing divisions in the *hmmr*$^{m/m}$ testis, resulting in partial rescue.

In summary, our data support the a/symmetric division hypothesis coupling apicobasal/planar divisions with differentiation/renewal, respectively, during the multiple stages of spermatogenesis.

Disruption of planar division and premature exit of undifferentiated GCs from the ST niche can be oncogenic

The atypia observed in the *hmmr*$^{m/m}$ testis is, at first glance, suggestive of RHAMM-dependent spindle defects. However, this is an unsatisfactory explanation, for several reasons. Atypia or aberrant spindle formation were not observed in spermatogonia, the most actively dividing GCs. Second, atypic cells were exclusively located in the ST lumen, but not in the area of high mitotic activity at the basal side of the ST epithelium. Third, atypia is a late onset phenotype (from 30 weeks-of-age), whereas other RHAMM truncation consequences, atrophy and hypofertility, are apparent already from 4 weeks-of-age. Indeed, although RHAMM is essential for acentrosomal spindle integrity (35, 50), it appears dispensable in centrosomal spindle formation and cell-cycle progression, as indicated by antibody (34), siRNA (Supplementary Fig. S5C; refs. 22, 51), or its genetically mediated (Supplementary Fig. S1B) disruption, including *in vivo* studies (20, 21).

Rather, our experiments provide three lines of evidence indicative of premature displacement of undifferentiated GCs from the ST niche into the adluminar area, in the absence of functional RHAMM: (i) spindle misalignment during what-should-be-planar divisions places an undifferentiated daughter GC apically; (ii) undifferentiated daughter GCs display symmetric segregation of PLZF, independently of the division plane orientation; (iii) undifferentiated spermatogonia accumulate in the adluminar space, where IGCN appears. These data raise two possibilities on the nature and properties of these cells. Some of the apically displaced undifferentiated GCs represent mutated dormant cells, which can initiate oncogenesis once they evade the suppressive ST epithelium. Alternatively, premature removal from the niche makes these cells vulnerable to secondary steps, required to enable their survival/growth outside the ST epithelium.

Displacement of cells from stem cell compartments and epithelia to the lumen can drive selection for survival and expansion (52–54), provoking hypothesis of a cell translocation mechanism that "allows sporadic cells to evade suppressive microenvironments and elicits clonal selection for survival and proliferative expansion outside the native niche of these cells" (54). We propose spindle misorientation during planar divisions as candidate for this role. Temporal and topological data from the *hmmr*$^{m/m}$ testis support this notion. First, atypia and IGCN are late-onset pathologies exclusively observed in the adluminal space. Second, ERK1/2 activation, which appears intrinsic in cell translocation from the epithelial layer to the lumen (54, 55), is elevated in the RHAMM heterozygocity (56) or the *hmmr*$^{m/m}$ truncation (21) context, but also in Sertoli cells in response to GC depletion (Supplementary Fig. S3I; ref. 57). Elevated ERK1/2 activation in the adluminal area would likely enhance the survival of displaced GCs outside their niche, thereby promoting seminoma. However, it is important to note that the ERK1/2 activation in the atrophic STs is not intrinsic to the RHAMM-expressing testicular cells (Supplementary Fig. S3I).

The relatively low prevalence of seminoma among atrophic hypo/infertile testes of *hmmr*$^{m/m}$ mice and hypo/infertile patients suggests that transition from precursor lesion to seminoma may require a secondary step to enable Sertoli-independent survival/growth of displaced GCs. It was not possible to evaluate whether deletion of p53 promotes seminoma development (*hmmr*$^{m/m}$; *Trp53*$^{-/-}$ mice die of lymphoma months before seminoma onset); moreover, the majority of TGCTs express wild-type p53 (8). Rather, the gain of isochromosome 12p, detected in up to 80% of seminomas but rarely in precursor lesions, has been proposed as a transition event (8). Alternatively, GC depletion (which precedes seminoma) probably limits the generation of spermatogonial stem cells with cancer-initiating potential, thus acting protectively against higher seminoma incidence.

In conclusion, our data show that mammalian male GCs perform stereotyped oriented divisions. Orientation failure results in premature displacement of undifferentiated GCs from the ST niche with two major consequences: (i) GC depletion, testicular atrophy, and hypofertility; (ii) cellular atypia in the ST lumen, IGCN, and seminoma. We propose that the stereotyped orientation of GC divisions regulates spermatogenesis. This process is orchestrated by spindle orientation and it critically depends on spindle-associated RHAMM. Furthermore, we propose that spindle misorientation is the initiating event for IGCN and seminoma development. We conclude that RHAMM orchestrates spermatogenesis and acts as a gatekeeper preventing seminoma development.

Disclosure of Potential Conflicts of Interest

No potential conflicts of interest were disclosed.

Authors' Contributions

Conception and design: H. Li, J. Moll, P. Herrlich, A. Ploubidou
Development of methodology: M.-L. Yaspo, M. Platzer, A. Ploubidou
Acquisition of data (provided animals, acquired and managed patients, provided facilities, etc.): H. Li, L. Frappart, J. Moll, A. Winkler, T. Kroll, M. Groth, H. Heuer, M. Platzer, K. Zatloukal, P. Herrlich, A. Ploubidou
Analysis and interpretation of data (e.g., statistical analysis, biostatistics, computational analysis): H. Li, L. Frappart, A. Winkler, T. Kroll, S. Taudien, M. Schütte, M.-L. Yaspo, B.M.H. Lange, M. Platzer, K. Zatloukal, P. Herrlich, A. Ploubidou
Writing, review, and/or revision of the manuscript: H. Li, L. Frappart, J. Moll, M.-L. Yaspo, B.M.H. Lange, K. Zatloukal, P. Herrlich, A. Ploubidou
Administrative, technical, or material support (i.e., reporting or organizing data, constructing databases): J. Hamann, I. Kufferath
Study supervision: A. Ploubidou

Acknowledgments

The support of the Animal, Functional Genomics, Histology and Imaging Core Facilities of the FLI are gratefully acknowledged, in particular Dominique Galendo and Mike Baldauf. We also thank Denise Reichmann for mouse colony maintenance and Dr. Lesley Ogilvie (Alacris) for her comments on the manuscript.

The costs of publication of this article were defrayed in part by the payment of page charges. This article must therefore be hereby marked *advertisement* in accordance with 18 U.S.C. Section 1734 solely to indicate this fact.

Received January 22, 2016; revised July 22, 2016; accepted July 27, 2016; published online August 19, 2016.

References

1. Gilbert D, Rapley E, Shipley J. Testicular GC tumours: predisposition genes and the male GC niche. Nat Rev Cancer 2011;11:278–88.
2. Moller H, Skakkebaek N. Risk of testicular cancer in subfertile men: case-control study. BMJ 1999;318:559–62.
3. Walsh TJ, Croughan MS, Schembri M, Chan JM, Turek PJ. Increased risk of testicular GC cancer among infertile men. Arch Intern Med 2009;169: 351–6.
4. Rapley EA, Turnbull C, Al Olama AA, Dermitzakis ET, Linger R, Huddart RA, et al. A genome-wide association study of testicular germ cell tumor. Nat Genet 2009;41:807–10.
5. Ruark E, Seal S, McDonald H, Zhang F, Elliot A, Lau K, et al. Identification of nine new susceptibility loci for testicular cancer, including variants near DAZL and PRDM14. Nat Genet 2013;45:686–9.
6. Chuang CC, Kanetsky PA, Wang Z, Hildebrandt MA, Koster R, Skotheim RI, et al. Meta-analysis identifies four new loci associated with testicular GC tumor. Nat Genet 2013;45:680–5.
7. Schumacher FR, Wang Z, Skotheim RI, Koster R, Chung CC, Hildebrandt MA, et al. Testicular GC tumor susceptibility associated with the UCK2 locus on chromosome 1q23. Hum Mol Genet 2013;22:2748–53.
8. Oosterhuis JW, Looijenga LH. Testicular GC tumours in a broader perspective. Nat Rev Cancer 2005;5:201–22.
9. de Rooji DG. Proliferation and differentiation of spermatogonial stem cells. Reproduction 2001;121:347–54.
10. Meng X, de Rooij DG, Westerdahl K, Saarma M, Sariola H. Promotion of seminomatous tumors by targeted overexpression of glial cell line-derived neurotrophic factor in mouse testis. Cancer Res 2001;61:3267–71.
11. Nakagawa T, Nabeshima Y, Yoshida S. Functional identification of the actual and potential stem cell compartments in mouse spermatogenesis. Dev Cell 2007;12:195–206.
12. Morin X, Bellaiche Y. Mitotic spindle orientation in asymmetric and symmetric cell divisions during animal development. Dev Cell 2011; 21:102–19.
13. Caussinus E, Gonzales C. Induction of tumor growth by altered stem-cell asymmetric division in *Drosophila melanogaster*. Nat Genet 2005;37: 1125–9.
14. Basto R, Brunk K, Vinadogrova T, Peel N, Franz A, Khodjakov A, et al. Centrosome amplification can initiate tumourigenesis in flies. Cell 2008;133:1032–42.
15. Quyn AJ, Appleton PL, Carey FA, Steele RJ, Barker N, Clevers H, et al. Spindle orientation bias in gut epithelial stem cell compartments is lost in precancerous tissue. Cell Stem Cell 2010;6:175–81.
16. Zimdahl B, Blevins A, Bajaj J, Konuma T, Weeks J, Koechlein CS, et al. Lis1 regulates asymmetric division in hematopoietic stem cells and in leukemia. Nat Genet 2014;46:245–52.
17. Lu MS, Johnston CA. Molecular pathways regulating mitotic spindle orientation in animal cells. Development 2013;140:1843–56.
18. Sohr S, Engeland K. RHAMM is differentially expressed in the cell cycle and downregulated by the tumor suppressor p53. Cell Cycle 2008;17:3448–60.
19. Assmann V, Jenkinson D, Marshall JF, Hart IR. The intracellular hyaluronan receptor RHAMM/IHABP interacts with microtubules and actin filaments. J Cell Sci 1999;112:3943–54.
20. Tolg C, Poon R, Fodde R, Turley EA, Alman BA. Genetic deletion of receptor for hyaluronan-mediated motility (Rhamm) attenuates the formation of aggressive fibromatosis (desmoid tumor). Oncogene 2003;22:6873–82.
21. Li H, Moll J, Winkler A, Frappart L, Brunet S, Hamann J, et al. RHAMM deficiency disrupts folliculogenesis resulting in female hypofertility. Biol Open 2015;4:562–71.
22. Dunsch AK, Hammond D, Lloyd J, Schermelleh L, Gruneberg UI, Barr FA. Dynein light chain 1 and a spindle-associated adaptor promote dynein asymmetry and spindle orientation. J Cell Biol 2012;198:1039–54.
23. Lagos-Cabre R, Moreno RD. Mitotic, but not meiotic, oriented cell divisions in rat spermatogenesis. Reproduction 2008;135:471–8.
24. Donehower LA, Harvey M, Slagle BL, McArthur MJ, Montgomery CA Jr, Butel JS, et al. Mice deficient for p53 are developmentally normal but susceptible to spontaneous tumours. Nature 1992;356:215–21.
25. Müller H, Schmidt D, Steinbrink S, Mirgorodskaya E, Lehmann V, Habermann K, et al. Proteomic and functional analysis of the mitotic *Drosophila* centrosome. EMBO J 2012;29:3344–57.
26. Kroll T, Schmidt D, Schwanitz G, Ahmad M, Hamann J, Schlosser C, et al. High-content microscopy analysis of subcellular structures: assay development and application to focal adhesion quantification. Curr Protoc Cytom 2016;77:12.43.1–44.
27. Assmann V, Gillett CE, Poulsom R, Ryder K, Hart IR, Hanby AM. The pattern of expression of the microtubule-binding protein RHAMM/IHABP in mammary carcinoma suggests a role in the invasive behaviour of tumour cells. J Pathol 2001;195:191–6.
28. Gust KM, Hofer MD, Perner SR, Kim R, Chinnaiyan AM, Varambally S, et al. RHAMM (CD168) is overexpressed at the protein level and may constitute an immunogenic antigen in advanced prostate cancer disease. Neoplasia 2009;11:956–63.
29. Koelzer VH, Huber B, Mele V, Iezzi G, Trippel M, Karamitopoulou E, et al. Expression of the hyaluronan-mediated motility receptor RHAMM in tumor budding cells identifies aggressive colorectal cancers. Hum Pathol 2015;46:1573–81.
30. He X, Liao W, Li Y, Wang Y, Chen Q, Jin J, et al. Upregulation of hyaluronan-mediated motility receptor in hepatocellular carcinoma predicts poor survival. Oncol Lett 2015;10:3639–46.
31. Tilghman J, Wu H, Sang Y, Shi X, Guerrero-Cazares H, Quinones-Hinojosa A, et al. HMMR maintains the stemness and tumorigenicity of glioblastoma stem-like cells. Cancer Res 2014;74:3168–79.
32. Mantripragada KK, Spurlock G, Kluwe L, Chuzhanova N, Ferner RE, Frayling IM, et al. High-resolution DNA copy number profiling of malignant peripheral nerve sheath tumors using targeted microarray-based comparative genomic hybridization. Clin Cancer Res 2008;14: 1015–24.
33. Burke AP, Mostofi FK. Placental alkaline phosphatase immunohistochemistry of intratubular malignant germ cells and associated testicular germ cell tumors. Hum Pathol 1988;19:663–70.
34. Maxwell CA, Keats JJ, Crainie M, Sun X, Yen T, Shibuya E, et al. RHAMM is a centrosomal protein that interacts with dynein and maintains spindle pole stability. Mol Biol Cell 2003;14:2262–76.
35. Joukov V, Groen AC, Prokhorova T, Gerson R, White E, Rodriguez A, et al. The BRCA1/BARD1 heterodimer modulates ran-dependent mitotic spindle assembly. Cell 2006;127:539–52.
36. Kornovski BS, McCoshen J, Kredentser J, Turley E. The regulation of sperm motility by a novel hyaluronan receptor. Fertil Steril 1994;61: 935–40.
37. Mitchell RT, E Camacho-Moll M, Macdonald J, Anderson RA, Kelnar CJ, O'Donnell M, et al. Intratubular germ cell neoplasia of the human testis: heterogeneous protein expression and relation to invasive potential. Mod Pathol 2014;27:1255–66.
38. Takubo K, Ohmura M, Azuma M, Nagamatsu G, Yamada W, Arai F, et al. Stem cell defects in ATM-deficient undifferentiated spermatogonia through DNA damage-induced cell-cycle arrest. Cell Stem Cell 2008;2:170–82.
39. Bazzi H, Anderson KV. Acentriolar mitosis activates a p53-dependent apoptosis pathway in the mouse embryo. Proc. Natl. Acad. Sci. USA 2014;111:E1491–500.
40. Faulkner SW, Leigh DA, Oosterhui JW, Roelofs H, Looijenga LH, Friedlander ML. Allelic losses in carcinoma in situ and testicular GC tumours of adolescents and adults: evidence suggestive of the linear progression model. Br J Cancer 2000;83:729–36.
41. Di Giammartino DC, Nishida K, Manley JL. Mechanisms and consequences of alternative polyadenylation. Mol Cell 2012;43:853–66.
42. Sartini BL, Wang H, Wang W, Millette CF, Kilpatrick DL. Pre-messenger RNA cleavage factor I (CFIm): potential role in alternative polyadenylation during spermatogenesis. Biol Reprod 2008;78:472–82.
43. Sketheim RI, Lothe RA. The testicular GC tumour genome. APMIS 2003; 111:136–50.
44. Masamha CP, Xia Z, Yang J, Albrecht TR, Li M, Shyu AB, et al. CFIm25 links alternative polyadenylation to glioblastoma tumour suppression. Nature 2014;510:412–6.
45. McGrail M, Hays TS. The microtubule motor cytoplasmic dynein is required for spindle orientation during germline cell divisions and oocyte differentiation in *Drosophila*. Development 1997;124:2409–19.
46. Luo J, Megee S, Dobrinski I. Asymmetric distribution of UCH-L1 in spermatogonia is associated with maintenance and differentiation of spermatogonial stem cells. J Cell Physiol 2009;220:460–68.
47. Wu M, Smith CL, Hall JA, Lee I, Luby-Phelps K, Tallquist MD. Epicardial spindle orientation controls cell entry into the myocardium. Dev Cell 2010;19:114–25.

Published OnlineFirst August 19, 2016; DOI: 10.1158/0008-5472.CAN-16-0179

48. Sato T, Aiyama Y, Ishii-Inagaki M, Hara K, Tsunekawa N, Harikae K, et al. Cyclical and patch-like GDNF distribution along the basal surface of Sertoli cells in mouse and hamster testes. PLoS One 2011;6:e28367.
49. Cicalese A, Bonizzi G, Pasi CE, Faretta M, Ronzoni S, Giulini B, et al. The tumor suppressor p53 regulates polarity of self-renewing divisions in mammary stem cells. Cell 2009;138:1083–95.
50. Groen AC, Cameron LA, Coughlin M, Miyamoto DT, Mitchison TJ, Ohi R. XRHAMM functions in ran-dependent microtubule nucleation and pole formation during anastral spindle assembly. Cur Biol 2004;14: 1801–11.
51. Neumann B, Walter T, Hériché JK, Bulkescher J, Erfle H, Conrad C, et al. Phenotypic profiling of the human genome by time-lapse microscopy reveals cell division genes. Nature 2010;464:721–7.
52. Vasiliev JM, Omelchenko T, Gelfand IM, Feder HH, Bonder EM. Rho overexpression leads to mitosis-associated detachment of cells from epithelial sheets: a link to the mechanism of cancer dissemination. Proc Natl Acad Sci USA 2004;101:12526–30.
53. Hogan C, Dupré-Crochet S, Norman M, Kajita M, Zimmermann C, Pelling AE, et al. Characterization of the interface between normal and transformed epithelial cells. Nat Cell Biol 2009;11:460–7.
54. Leung CT, Brugge JS. Outgrowth of single oncogene-expressing cells from suppressive epithelial environments. Nature 2012;482:410–3.
55. Tang N, Marshall WF, McMahon M, Metzger RJ, Martin GR. Control of mitotic spindle angle by the RAS-regulated ERK1/2 pathway determines lung tube shape. Science 2009;333:342–5.
56. Jiang J, Mohan P, Maxwell CA. The cytoskeletal protein RHAMM and ERK1/2 activity maintain the pluripotency of murine embryonic stem cells. PLoS One 2013;8:e73548.
57. Hasegawa K, Namekawa SH, Saga Y. MEK/ERK signaling directly and indirectly contributes to the cyclical self-renewal of spermatogonial stem cells. Stem Cells 2013;31:2517–27.

Published OnlineFirst August 19, 2016; DOI: 10.1158/0008-5472.CAN-16-0179

Cancer Research
The Journal of Cancer Research (1916–1930) | The American Journal of Cancer (1931–1940)

AACR American Association for Cancer Research

Impaired Planar Germ Cell Division in the Testis, Caused by Dissociation of RHAMM from the Spindle, Results in Hypofertility and Seminoma

Huaibiao Li, Lucien Frappart, Jürgen Moll, et al.

Cancer Res 2016;76:6382-6395. Published OnlineFirst August 19, 2016.